ACS Photonics

Letter

Cite This: ACS Photonics 2019, 6, 3070−3075

pubs.acs.org/journal/apchd5

Systematic Design of the Color Point of a White LED

Maryna L. Meretska,[†,§] Gilles Vissenberg,[‡] Ad Lagendijk,[†] Wilbert L. IJzerman,[*,‡,¶] and Willem L. Vos[*,†]

[†]Complex Photonic Systems (COPS), MESA+ Institute for Nanotechnology, University of Twente, P.O. Box 217, 7500 AE Enschede, The Netherlands

[‡]Signify NV, High Tech Campus 7, 5656 AE Eindhoven, The Netherlands

[¶]Department of Mathematics and Computer Science, Eindhoven University of Technology, 5600 MB Eindhoven, The Netherlands

Supporting Information

ABSTRACT: Lighting is a crucial technology that is used in our daily lives. The introduction of the white light emitting diode (LED), which consists of a blue LED combined with a phosphor layer, greatly reduces the energy consumption for lighting. Despite the fast-growing market, white LEDs are still being designed with slow, numerical, trial-and-error methods. Here we introduce a radically new design principle that is based on an analytical model instead of a numerical approach. Our model predicts the white LED's color point for any combination of design parameters. In addition, our model provides the reflection and transmission coefficients of the scattered and re-emitted light intensities, as well as the energy density distribution inside the LED. To validate our model, we have performed extensive experiments on an emblematic white LED and found excellent agreement. Our model provides for a fast and efficient design, resulting in reductions of both design and production costs.

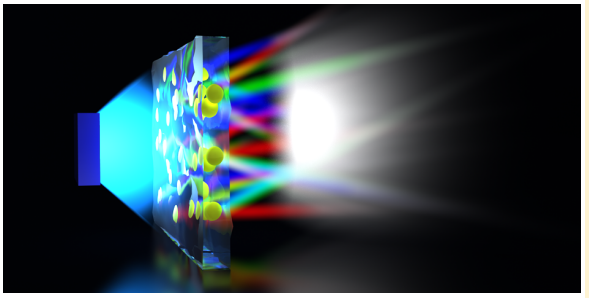

KEYWORDS: *white LED, color point, phosphor, scattering, absorption, radiative transport*

The main characteristics of white light sources are their color point[1] and efficiency. The color point is described using two independent chromaticity parameters that span the color space.[2,3] The color point of any light source is defined by the spectrum that it emits. Optical designers currently use numerical simulations, often based on Monte Carlo ray tracing techniques,[4,5] to extract the color point, given the design parameters of the white light source. To target a specific color point, optical designers have to use these simulations for each chosen set of design parameters. Unfortunately simulation methods are very slow, and consequently only a small part of the design parameter space can be explored. Hence the design of a white LED relies on the experience of the optical designer rather than on a systematic exploration of the full design parameter space.

An important class of white light sources is white LEDs, which possess numerous advantages over conventional sources, such as incandescent lamps or discharge lamps. White LEDs are among the most energy efficient sources,[6,7] they are mechanically robust and thermally stable, they possess good temporal stability, and they have a long lifetime.[8,9] To systematically design the color point of a white LED,[10,11] algorithms are needed that are much faster than ray tracing techniques.

A typical white LED consists of a blue semiconductor LED[12−14] in combination with a phosphor layer,[10] which consists of a dielectric matrix with a density ρ of phosphor microparticles (see Figure 1). Part of the blue light is transmitted through the phosphor layer, and part is absorbed and re-emitted in the red and green part of the spectrum to yield the desired white light that illuminates a targeted object or space. The relative amounts of scattered and re-emitted light define the color point of a white LED. To adjust the color point, several design parameters are available, such as the

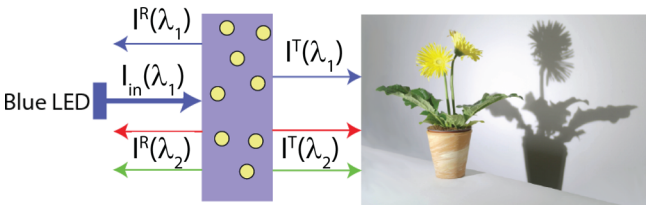

Figure 1. Model of light propagation in a white LED slab. Blue excitation light with intensity $I_{in}(\lambda_1)$ that originates from the blue LED is shone on the phosphor slab with thickness L. The phosphor slab contains phosphor microparticles that are represented by yellow circles. $I^T(\lambda_1)$ is the scattered transmitted intensity, $I^R(\lambda_1)$ is the scattered reflected intensity, $I^T(\lambda_2)$ is the transmitted re-emitted intensity, and $I^R(\lambda_2)$ is the reflected re-emitted intensity, both per bandwidth of the detector at λ_2. The mixture of transmitted red, green, and blue light illuminates the object, such as a flower.

Received: January 30, 2019
Published: July 26, 2019

DOI: 10.1021/acsphotonics.9b00173
ACS Photonics 2019, 6, 3070−3075

phosphor layer thickness L, the phosphor particle density ρ, the phosphor type, the type of blue LED, and the particle density of the additional scattering elements. In this paper, we introduce an extremely fast and analytic computational tool, based on the so-called P3 approximation to the radiative transfer equation (see Methods), to predict the color point of a white LED starting from the chosen design parameters and, conversely, to infer the design parameters of a white LED beginning from a targeted color point. In our case the inverse problem does not require an iteration procedure for each new design cycle. Given the speed of our tool, we can generate—once and for all—a look-up table for the whole parameter space available to engineers.

The core of our method is to calculate the spatial light energy distribution of the scattered and of the re-emitted light inside a white LED. From this spatial profile the reflection and transmission coefficients can be obtained. Our model does not involve any assumption regarding the physical processes that result in scattering of light and does not suffer from any limitation imposed on the wavelength of the excitation light. Hence it can be applied to any type of scattering particles including different kinds of phosphors or even quantum dots.

Studying the sensitivity of the energy distribution to changing design parameters gives much insight and can be used to design more efficient and more robust LEDs. For instance, it was recently demonstrated that the functioning of phosphor layers could degrade substantially due to thermal effects.[15] In addition, heat generated from the phosphor particles (due to Stokes losses) can cause damage to the polymer matrix.[16] Degradation due to heating can be explained by inspecting the internal energy distribution and can even be prevented by choosing design parameters that avoid hot spots. Nonlinear effects, caused by peaks in the energy profile, lead to quenching and lifetime degradation of a white LED. For high-power laser-driven phosphor-based white LEDs that are used for outdoor lighting or car headlamps,[17] engineering of the energy distribution is crucial to minimize the effect of quenching.[18] In more exotic cases, such as quantum-dot-based or dye-based white LEDs,[19] hot spots cause bleaching of the quantum dots or the dye.

Our analytical model generates all light fluxes, scattered and re-emitted, emanating from a white LED at all wavelengths (see Figure 1). In addition the corresponding energy densities inside the LED are a natural result of our approach. The transmission $T_{exc}(\lambda_1)$ and reflection $R_{exc}(\lambda_1)$ coefficients of the excitation light that is partly scattered are analytically calculated using the P3 approximation to the radiative transfer equation (see Methods). To solve the P3 approximation for the scattered light, the following properties of the phosphors are needed: the scattering cross section $\sigma_s(\lambda_1)$, the absorption cross section $\sigma_a(\lambda_1)$, the anisotropy factor $\mu(\lambda_1)$, the thickness of the phosphor layer d, and the particle density ρ of the phosphor particles. The concentration and the slab thickness are chosen by the optical designer, and the other three parameters can be obtained for the whole visible spectral range from experiments as described elsewhere[20−22] or using Mie theory.[23] We obtain the spatial energy distribution $U_{exc}(\lambda_1,z)$ of the excitation light inside the slab,[24] the transmission and reflection coefficients from the P3 approximation. To obtain the re-emitted intensities, the average energy density of the excitation light $U_{exc}(\lambda_1,z)$ is used as a source function for the transport of the re-emitted light. At position z the excitation intensity is proportional to $U_{exc}(\lambda_1,z)$, and the power of the re-emitted light at wavelength λ_2 is proportional to $q(\lambda_1)$ $U_{exc}(\lambda_1,z)$ $F(\lambda_2)$, where $F(\lambda_2)$ is the normalized re-emission (fluorescence) spectrum and $q(\lambda_1)$ is the quantum efficiency. Both the normalized re-emission spectrum and the quantum efficiency can be extracted from experiments and are known for many phosphors.[25]

The scattering of the re-emitted light by a particle is characterized by the scattering cross section $\sigma_s(\lambda_2)$, the anisotropy factor $\mu(\lambda_2)$, and the absorption cross section $\sigma_a(\lambda_2)$. Application of the P3 approximation to the transport of the re-emitted intensity generates both the energy density of the re-emitted light, $U_{rem}(\lambda_2,z)$, and also the transmission and the reflection of the re-emitted light. We introduce the differential re-emitted transmission intensity $I^T_{rem}(\lambda_1,\lambda_2)\ d\lambda_2$ and reflection intensity $I^R_{rem}(\lambda_1,\lambda_2)\ d\lambda_2$ and use them to define the total re-emitted intensities by integrating the differential intensities over the re-emission spectrum: $\int I^T_{rem}(\lambda_1,\lambda_2)\ d\lambda_2$ and $\int I^R_{rem}(\lambda_1,\lambda_2)\ d\lambda_2$. When normalizing the total re-emitted intensities with the incident intensity, we obtain dimensionless coefficients that can be easily compared to experiments: $T_{rem}(\lambda_1) \equiv \int I^T_{rem}(\lambda_1,\lambda_2)\ d\lambda_2/I_{in}(\lambda_1)$, and $R_{rem}(\lambda_1) \equiv \int I^R_{rem}(\lambda_1,\lambda_2)\ d\lambda_2/I_{in}(\lambda_1)$.

RESULTS AND DISCUSSION

To demonstrate the validity of our tool, we experimentally study light propagation through a representative white LED and interpret the results using our model. The LED consists of a polymer diffuser plate containing YAG:Ce^{3+} phosphor microparticles. The refractive index of the diffuser plates is n = 1.4, and the plate thickness L = 1.98 ± 0.02 mm. The absorption and the emission spectra of the phosphor are discussed elsewhere.[26] The phosphor particle density ρ ranges from 1 wt % to 8 wt %. A narrow-band light source, tunable from 420 to 800 nm, with intensity $I_{in}(\lambda_1)$ illuminates the samples at a wavelength λ_1.[26] The incident light is scattered, absorbed, and re-emitted. The transmitted and reflected intensities are separately collected with an integrating sphere and detected with a fiber spectrometer. The typical signal of our model white LED is shown in Figure 2. The sharp peak at λ_1 = 475 nm originates from the light source and contributes to the scattered light intensities. The broad peak between 490 and 700 nm consists of the re-emitted light.

From the experiment we infer the following quantities that are compared with the predictions of our model: the scattered transmission coefficient $T_{exc}(\lambda_1)$, the scattered reflection

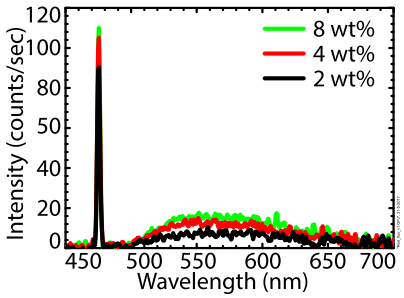

Figure 2. Typical measured signal of the model white LED. Observed emission from a white LED in reflection when excited with λ_1 = 475 nm narrow-band light, for three different phosphor concentrations. The sharp peak at 475 nm is the scattered incident light in reflection, and the broad peak between 490 and 700 nm is light re-emitted by the phosphor.

DOI: 10.1021/acsphotonics.9b00173
ACS Photonics 2019, 6, 3070−3075

coefficient $R_{exc}(\lambda_1)$, the total transmission coefficient of re-emitted light $T_{rem}(\lambda_1)$, and the total reflection coefficient of re-emitted light $R_{rem}(\lambda_1)$. The total re-emitted transmission coefficient $T_{rem}(\lambda_1)$ and the total re-emitted reflection coefficient $T_{rem}(\lambda_1)$ are obtained by integrating the differential transmission and reflection coefficients over λ_2 from 490 to 700 nm by binning the wavelength in 841 points. The experimental results for the scattered blue light are shown in Figure 3. The transmission $T_{exc}(\lambda_1)$ of the scattered light

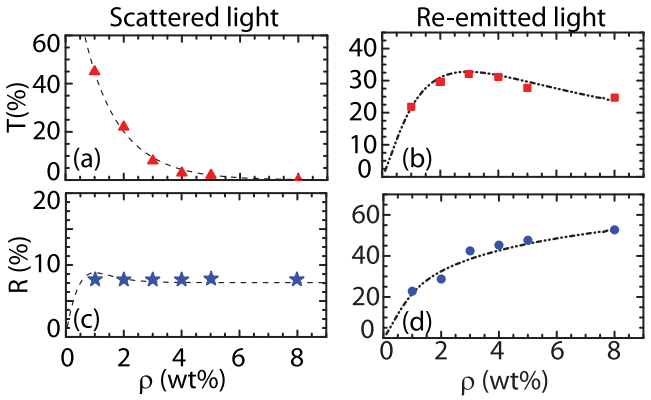

Figure 3. Transmission and reflection of a model white LED as a function of phosphor particle density at λ_1 = 475 nm. (a) Dashed line represents the calculated total transmission coefficient of the scattered light; triangles represent the measured coefficient. (b) Dash-dot-dot line represents the calculated total transmission coefficient of the re-emitted light; squares represent the measured coefficients. (c) Dashed line represents the calculated reflection coefficient of the scattered light; stars represent the measured coefficient. (d) Dashed-dot line represents the calculated reflection coefficient of the re-emitted light; circles represent the measured coefficient. The error bars of the experiment are within the symbol size.

reveals a sharp decrease with the phosphor particle density ρ as a result of scattering and strong absorption of the incident light. The reflection $R_{exc}(\lambda_1)$ hardly varies with the phosphor particle density due to absorption; if the phosphor did not absorb light, we would have observed growth of the reflection with the increasing phosphor particle density, but the absorption counters this growth. The measured total transmission coefficient $T_{rem}(\lambda_1)$ and total reflection coefficient $R_{rem}(\lambda_1)$ of the re-emitted light are also shown in Figure 3(a)−(d). At low particle density, the re-emitted light intensity $R_{rem}(\lambda_1)$ increases with the phosphor particle density, because more phosphors absorb more light. A saturation occurs at ρ = 3.3 wt %, because a further increase of the particle density increases the probability of incident photons being absorbed very close to the entrance surface of the scattering material. When most photons are absorbed near the entrance surface, most re-emitted photons leave through the entrance surface, corresponding to a decrease of the transmitted re-emitted flux and an increase of the reflected re-emitted flux $R_{rem}(\lambda_1)$. The color points for the measured data are plotted in the color space in Figure 4. The experimentally determined quantum yield can be obtained from $q(\lambda_1) = \{T_{rem}(\lambda_1) + R_{rem}(\lambda_1)\}/\{1 - T_{rmex}(\lambda_1) - R_{exc}(\lambda_1)\}$ and is presented in Figure 5.

Model Validation. The results of our analytical model for the transmissions $T_{exc}(\lambda_1)$ and $T_{rem}(\lambda_1)$ and the reflections $R_{exc}(\lambda_1)$ and $R_{rem}(\lambda_1)$ are shown as a function of particle density ρ in Figure 3(a)−(d), together with our experimental data. We find an excellent agreement between experiment and

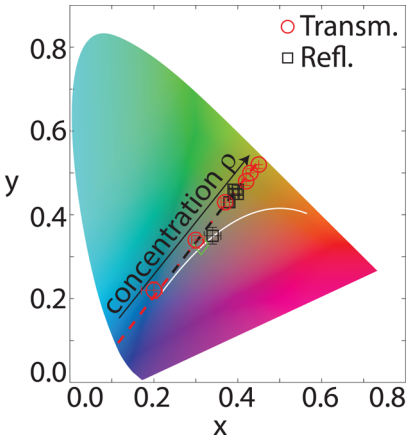

Figure 4. Color point of a white LED. Circles (transmission) and squares (reflection) are our experimental data points for the wavelength λ_1 = 475 nm (see Supporting Information, Table S1). Red and black dashed lines represent predicted color points as a function of the phosphor particle density ρ (1 wt % to 8 wt %) for transmitted and reflected light, respectively (see Figure 3). The green diamond indicates the most widely used standardized white light spectrum, the D65 spectrum.

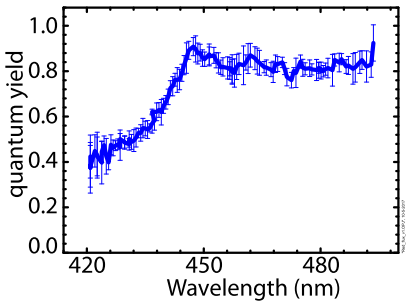

Figure 5. Quantum yield of YAG:Ce^{3+}. Quantum yield as a function of the excitation wavelength λ_1 as extracted from our measurements.

our model. To explain the behavior of the $T_{rem}(\lambda_1)$ and $R_{rem}(\lambda_1)$ as a function of phosphor particle density, we plot the absorbed power $4\pi\rho\sigma_a U_{exc}(z)$ as a function of depth inside the scattering medium in Figure 6. When the particle density of the phosphor particles is low (ρ = 2), the absorbed power is distributed almost uniformly across the sample. When considering for this case a thin representative layer positioned at $z = z_B = L/3$ the re-emitted light generated from this layer will contribute mostly to the re-emitted reflection $R_{rem}(\lambda_1)$,

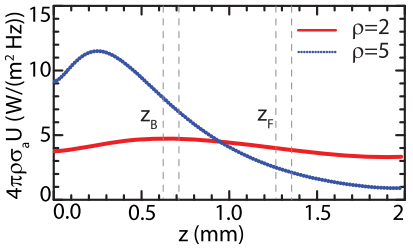

Figure 6. Energy density profile inside model white LED. Lines represent the calculated average intensity $U(z)$ of the excitation (blue) light as a function of depth inside the sample for two different phosphor particle particle densities ρ. Two representative thin layers, positioned respectively at $z_B = L/3$ and $z_F = 2L/3$, are indicated in the figure and are discussed in the text; L is the thickness of the sample.

DOI: 10.1021/acsphotonics.9b00173
ACS Photonics 2019, 6, 3070−3075

because light that is re-emitted in the backward direction in this layer will experience less scattering compared to the forward re-emitted light. For a second thin representative layer, positioned at $z = z_F = 2L/3$, the re-emitted light will mostly contribute to the transmission $T_{rem}(\lambda_1)$ for the same reason.

When the phosphor particle density is high ($\rho = 5$), the intensity is mostly absorbed near the entrance surface of the slab; hence the layer at z_B will contribute a higher intensity in the backward direction compared to the low particle density case, and the layer at z_F will contribute less intensity in transmission $T_{rem}(\lambda_1)$ compared to the low particle density case. This interplay results in the peak in transmission $T_{rem}(\lambda_1)$ at $\rho = 3.3$ wt % and a steady increase of reflection $R_{rem}(\lambda_1)$ with particle density ρ (see Figure 3).

The color points for the measured data and our model are plotted in the color space in Figure 4 and show excellent agreement. The theoretical curves indicate all possible color points that can be achieved with the given YAG:Ce^{3+} phosphor when the particle density ρ is changed. The observed dependence of the color point on particle density is remarkably linear given the observation in Figure 3 that the scattered and re-emitted light intensities depend nonlinearly on the particle density. The color point linearly shifts to the yellow part of the color space with increasing particle density for both the transmitted and reflected light, as shown in Figure 4. The reason is that a higher particle density enhances the absorption of blue light, thereby increasing the yield of re-emitted yellow light. The re-emitted flux has qualitatively a similar dependence on both the particle density and the thickness of the polymer layer. If the refractive index of the polymer is varied from 1.4 to 1.5, as is typical for industrially used materials, the re-emitted flux is robust, as it increases by less than 4%.

In a widely used design to improve its efficiency, a white LED contains an additional mirror that reflects the back-scattered flux.[10] Our model can be easily extended to include such a mirror. As an example, we consider a silver mirror with a reflectivity of 99% and assume the quantum efficiency of the phosphor to be $q = 1$. With such a mirror, we calculate that the re-emitted flux increases by up to 40% compared to the design without mirror, thus confirming the advantage of the mirror in the design.

To calculate the color point of white LED with a broadband excitation, the spectrum should be partitioned in a number of narrow frequency bands that are each separately calculated. The final result is then obtained by summing the contributions of all the narrow frequency bands. An interesting future extension for our model will be to include the effects of self-absorption.

CONCLUSIONS

We have developed an analytic and very fast model that can revolutionize white LED design. Our model, based on an analytic algorithm without adjustable parameters, provides a simple design tool. The main advantage of our model is its extremely short execution time (see Methods). Given a specific set of transport parameters, all fluxes are calculated extremely fast, notably in comparison to simulations or ray tracing. Moreover, given the increased calculation speed, the performance of any desired LED can be readily obtained by exploring an unprecedentedly large parameter space.

Our design principle is based on calculating the spatial light energy density. This property is crucial in designing a white LED, as it not only allows predicting the color of a white LED but also supplies information about mitigation of heat generation inside the phosphor layer. Knowledge of a spatial distribution of heat produced by the phosphor allows calculating thermal quenching and lifetime performance of a white LED, as heat from phosphors causes damage to the polymer by decreasing its performance. Our design method can be applied to design traditional phosphor-based white LEDs, but also to more modern systems such as laser-driven white LEDs and white LEDs that contain quantum dots. While our current solution provides a single-layer description of the light propagation and re-emission, the extension to more complex geometries typically employed in white LED design seems well feasible. Indeed, the extension to multiple layers, albeit without the major complication of re-emission, has already been reported.[27] Our approach will increase the design efficiency by avoiding recurring design efforts and decrease the cost of ownership of white LEDs units for worldwide users and is already being put to use by engineers in industry.

METHODS

P3 Approximation to Radiative Transfer. The key property to calculate in radiative transport is the specific intensity $I(r, \hat{s})$, which represents the average power flux density per unit frequency and per unit solid angle for direction $\hat{s}$ at position r. To separate the coupled dependency on the variables r and $\hat{s}$, one expands the intensity into a product of functions that depend on either r or on $\hat{s}$:

$$I(r, \hat{s}) = \sum_{l=0}^{\mathcal{L}} \sum_{m=-l}^{l} \psi_{lm}(r)\, Y_{lm}(\hat{s}) \tag{1}$$

where Y_{lm} are the spherical harmonics and the functions ψ_{lm} are determined by the boundary conditions. In principle the expansion is exact if we take $\mathcal{L}$ to infinity. When limiting $\mathcal{L}$ to finite N, the expansion is called the PN approximation. It appears that only odd N gives sensible results.[28] In media with strong absorption the P1 approximation—also known as the diffusion approximation—is known to fail.[29] For the diffusion approximation to be valid, the spatial gradients of the specific intensity have to be small. With strong absorption, this gradient becomes too large, as absorption induces an exponential decay with a decay length less than the scattering mean free path. In these cases, one has to resort to the P3 approximation[30−33] to the radiative transfer equation.[34] Only in exceptional cases, characterized by high absorption combined with high scattering anisotropy, have higher approximations—like the complex P5 approximation—been invoked. The derivation of the P3 approximation for several geometries has been published before.[30−34] The formulas for the P3 approximation can be obtained by simply using symbolic manipulation by, for example, Mathematica. Since the P3 equations for the slab geometry have not been explicitly published as far as we know, we fully provide them in the Supporting Information.

Comparison with Alternative Models. The alternative computational methods that can compete with our model regarding accuracy but not regarding speed are Monte Carlo simulations and the adding−doubling method.[35,36] The adding−doubling method consists of approximating the transport properties of a very thin, hypothetical, layer very accurately and then further doubling the thin layer again and again until the required layer thickness is reached. Any doubling cycle requires numerical matrix inversion and angular

DOI: 10.1021/acsphotonics.9b00173
ACS Photonics 2019, 6, 3070−3075

integrals, approximated by discretizing the angular coordinates and using a numerical quadrature method such as the Gaussian−Legendre quadrature. The adding−doubling method has been very successful in describing the optical properties of biological tissue.[36] To apply the adding−doubling method to light transport in LEDs, it has to be generalized to include the substantial complication of re-emission.[37] Very recently this more complex adding−doubling method was applied to LED design.[38] In this generalized form the numerical calculation of transmission and reflection has to be done for each excitation wavelength λ_1 and for each re-emission wavelength λ_2. According to Leyre et al.,[37] a ray tracing calculation on a single $\{\lambda_1, \lambda_2\}$ pair takes several hours on a standard PC, whereas the adding−doubling method takes only about 35 s. For the design of a LED, however, the light transport for the whole re-emission spectrum has to be calculated, implying the discretization of λ_2 in at least 100 points. This full spectral scan of the re-emitted light with the adding-doubling method would take on the order of an hour. With our analytic method on the other hand, where we bin λ_2 in no less than 841 points, the *whole* scattering and re-emission calculation with Mathematica takes about 0.75 s. As a matter of fact the integration over the re-emission spectrum only implies a small additional overhead, and even a full excitation scan combined each time with a full re-emission scan would take only a few minutes. To obtain the energy distribution inside an LED using the adding−doubling method is *in principle* possible, but cumbersome and has, to the best of our knowledge, not yet been reported.

■ ASSOCIATED CONTENT

Supporting Information

The Supporting Information is available free of charge on the ACS Publications website at DOI: 10.1021/acsphotonics.9b00173.

Additional information (PDF)

■ AUTHOR INFORMATION

Corresponding Authors

*E-mail: wilbert.ijzerman@signify.com.
*E-mail: w.l.vos@utwente.nl.

ORCID

Maryna L. Meretska: 0000-0001-8749-9374
Willem L. Vos: 0000-0003-3066-859X

Present Address

[§]Harvard John A. Paulson School of Engineering and Applied Sciences, Harvard University, Cambridge, Massachusetts 02138, United States.

Notes

The authors declare no competing financial interest.

■ ACKNOWLEDGMENTS

It is a great pleasure to thank Jan Jansen from Philips Lighting for sample fabrication, Cornelis Harteveld for technical support, Diana Grishina, Oluwafemi Ojambati, Ravitej Uppu, and Shakeeb Bin Hasan for useful discussions, and Nono Groenen for helping with Figure [1,] and the TOC figure. This work was supported by the Dutch Technology Foundation STW (contract no. 11985) and by the NWO-FOM program "Stirring of Light!" and by the NWO-TTW program "Free form scattering optics" and by NWO Rubicon Grant 019.173EN.010, by the Dutch Funding Agency NWO and by MESA+ Applied Nanophotonics (ANP).

■ REFERENCES

(1) Malacara, D. *Color Vision and Colorimetry: Theory and Applications*; SPIE: WA, 2011.
(2) Smith, T.; Guild, J. The C.I.E. Colourimetric Standards and Their Use. *Trans. Opt. Soc.* **1932**, *33*, 73.
(3) de l'Eclairage, C. I. *Proceedings 8th Session*; Cambridge University Press: Cambridge, 1932.
(4) Luo, H.; Jong, K. K.; Schubert, E. F.; Cho, J.; Sone, C.; Park, Y. Analysis of High-Power Packages for Phosphor-Based White-Light-Emitting Diodes. *Appl. Phys. Lett.* **2005**, *86*, 243505.
(5) Tran, N. T.; Shi, F. G. Studies of Phosphor Concentration and Thickness for Phosphor-Based White Light-Emitting-Diodes. *J. Lightwave Technol.* **2008**, *26*, 3556−3559.
(6) de Almeida, A.; Fonseca, P.; Schlomann, B.; Feilberg, N. Characterization of the Household Electricity Consumption in the EU, Potential Energy Savings and Specific Policy Recommendations. *Ener. Build.* **2011**, *43*, 1884−1894.
(7) Danish Energy Agency *Energy Piano CLASP*; see http://clasp.ngo//media/Files/SLDocuments/2015/DEA%20-%20CLASP%20Report%20on%20European%20LED%20Market_final.ashx, 2016; accessed Oct 24, 2017.
(8) Haitz's Law. *Nat. Photonics* **2007**, *1*, 23.
(9) Pulli, T.; Donsberg, T.; Poikonen, T.; Manoocheri, F.; Karha, P.; Ikonen, E. Advantages of White LED Lamps and New Detector Technology in Photometry. *Light: Sci. Appl.* **2015**, *4*, No. e332.
(10) Schubert, E. F. *Light-Emitting Diodes*, 2nd ed.; Cambridge University Press: London, 2006.
(11) Horiuchi, N. Light-Emitting Diodes: Natural White Light. *Nat. Photonics* **2010**, *4*, 738.
(12) Nakamura, S.; Iwasa, N.; Senoh, M.; Mukai, T. Hole Compensation Mechanism of P-Type GaN Films. *Jpn. J. Appl. Phys.* **1992**, *31*, 1258.
(13) Amano, H.; Kito, M.; Hiramatsu, K.; Akasaki, I. P-Type Conduction in Mg-Doped GaN Treated with Low-Energy Electron Beam Irradiation. *Jpn. J. Appl. Phys.* **1989**, *28*, L2112.
(14) Pimputkar, S.; Speck, J. S.; DenBaars, S. P.; Nakamura, S. Prospects for LED Lighting. *Nat. Photonics* **2009**, *3*, 180.
(15) Tan, C. M.; Singh, P.; Zhao, W.; Kuo, H.-C. Physical Limitations of Phosphor Layer Thickness and Concentration for White LEDs. *Sci. Rep.* **2018**, *8*, 2452.
(16) Singh, P.; Tan, C. M. Degradation Physics of High Power LEDs in Outdoor Environment and the Role of Phosphor in the Degradation Process. *Sci. Rep.* **2016**, *6*, 24052.
(17) Song, Y. H.; Ji, E. K.; Jeong, B. W.; Jung, M. K.; Kim, E. Y.; Yoon, D. H. High Power Laser-Driven Ceramic Phosphor Plate for Outstanding Efficient White Light Conversion in Application of Automotive Lighting. *Sci. Rep.* **2016**, *6*, 31206.
(18) Kim, Y. H.; Arunkumar, P.; Kim, B. Y.; Unithrattil, S.; Kim, E.; Moon, S.-H.; Hyun, J. Y.; Kim, K. H.; Lee, D.; Lee, J.-S.; Im, W. B. A Zero-Thermal-Quenching Phosphor. *Nat. Mater.* **2017**, *16*, 543-550.
(19) Martino, D. D.; Beverina, L.; Sassi, M.; Brovelli, S.; Tubino, R.; Meinardi, F. Straightforward Fabrication of Stable White LEDs by Embedding of Inorganic UV-LEDs into Bulk Polymerized Polymethyl-Methacrylate Doped with Organic Dyes. *Sci. Rep.* **2015**, *4*, 4400.
(20) Vos, W. L.; Tukker, T. W.; Mosk, A. P.; Lagendijk, A.; IJzerman, W. L. Broadband Mean Free Path of Diffuse Light in Polydisperse Ensembles of Scatterers for White Light-Emitting Diode Lighting. *Appl. Opt.* **2013**, *52*, 2602−2609.
(21) Gaonkar, H. A.; Dinesh, K.; Rajagopal, R.; Arindam, R. Decoupling Scattering and Absorption of Turbid Samples Using a Simple Empirical Relation between Coefficients of the Kubelka-Munk and Radiative Transfer Theories. *Appl. Opt.* **2014**, *53*, 2892−2898.
(22) Meretska, M. L.; Uppu, R.; Vissenberg, G.; Lagendijk, A.; IJzerman, W. L.; Vos, W. L. Analytical Modeling of Light Transport in

DOI: 10.1021/acsphotonics.9b00173
ACS Photonics 2019, 6, 3070−3075

Scattering Materials with Strong Absorption. *Opt. Express* **2017**, *25*, A906−A921.
(23) Bohren, F. C.; Huffman, R. D. *Absorption and Scattering of Light by Small Particles*; Wiley: New York, 1983.
(24) Ishimaru, A. *Wave Propagation and Scattering in Random Media*; Academic, Vols. *I and II*, 1978.
(25) Smet, P. F.; Parmentier, A. B.; Poelman, D. Selecting Conversion Phosphors for White Light-Emitting Diodes. *J. Electrochem. Soc.* **2011**, *158*, R37−R54.
(26) Meretska, M. L.; Lagendijk, A.; Thyrrestrup, H.; Mosk, A. P.; IJzerman, W. L.; Vos, W. L. How to Distinguish Elastically Scattered Light from Stokes Shifted Light for Solid-State Lighting? *J. Appl. Phys.* **2016**, *119*, 093102.
(27) Liemert, A.; Reitzle, D.; Kienle, A. Analytical Solutions of the Radiative Transport Equation for Turbid and Fluorescent Layered Media. *Sci. Rep.* **2017**, *7*, 3819.
(28) Larsen, J. *Foundations of High-Energy-Density Physics: Physical Processes of Matter at Extreme Conditions*; Cambridge University Press: New York, 2017.
(29) Meretska, M. L.; Uppu, R.; Lagendijk, A.; Vos, W. L. Universal Validity Ranges of Diffusion Theory for Light and Other Electromagnetic Waves. arxiv.org/abs/1904.02784, **2019**.
(30) Liemert, A.; Kienle, A. Explicit Solutions of the Radiative Transport Equation in the P3 approximation. *Med. Phys.* **2014**, *41*, 3819.
(31) Star, W. M. Comparing the P3-approximation with DiffusionTheory and the with Monte Carlo Calculations of Light Propogation in a Slab Geometry. *Proc. SPIE* **1988**, 146.
(32) Dickey, D.; Barajas, O.; Brown, K.; Tulip, J.; Moore, R. B. Radiance Modelling Using the P3 Approximation. *Phys. Med. Biol.* **1998**, *43*, 3559.
(33) Klose, A. D.; Larsen, E. W. Light Transport in Biological Tissue based on the Simplified Spherical Harmonics Equations. *J. Comput. Phys.* **2006**, *220*, 441.
(34) Chandrasekhar, S. *Radiative Transfer*; Dover Publications Inc.: New York, 1960.
(35) van de Hulst, H. *Multiple Light Scattering*; Academic, Vol. *I*, 1980.
(36) Prahl, S. A.; van Gemert, M. J. C.; Welch, A. J. Determining the Optical Properties of Turbid Media by Using the Adding-Doubling method. *Appl. Opt.* **1993**, *32*, 559−568.
(37) Leyre, S.; Durinck, G.; Van Giel, B.; Saeys, W.; Hofkens, J.; Deconinck, G.; Hanselaer, P. Extended Adding-Doubling Method for Fluorescent Applications. *Opt. Express* **2012**, *20*, 17856.
(38) Ryckaert, J.; Leyre, S.; Hanselaer, P.; Meuret, Y. Determination of the Optimal Amount of Scattering in a Wavelength Conversion Plate for White LEDs. *Opt. Express* **2015**, *23*, A1629.

DOI: 10.1021/acsphotonics.9b00173
ACS Photonics 2019, 6, 3070−3075